doi:10.1093/brain/awm149 *Brain* (2007), **130**, 2354–2366

Interictal high-frequency oscillations (100–500 Hz) in the intracerebral EEG of epileptic patients

Elena Urrestarazu,* Rahul Chander, François Dubeau and Jean Gotman

Montreal Neurological Institute and Hospital, McGill University, Montréal (Québec), Canada
*Present address: University of Navarra, Pamplona, Spain

Correspondence to: Jean Gotman, PhD, Montreal Neurological Institute and Hospital, 3801 University Street, Montréal (Québec), Canada H3A 2B4.
E-mail: jean.gotman@mcgill.ca

Interictal fast oscillations between 100 and 500 Hz have been reported in signals recorded from implanted microelectrodes in epileptic patients and experimental rat models. Oscillations between 250 and 500 Hz, or fast ripples (FR), appeared related to the epileptic focus whereas ripples (80–200 Hz) were not. We report high-frequency oscillations recorded with intracranial macroelectrodes in seven patients with refractory focal epilepsy during slow-wave sleep. We characterize the relation of fast oscillations to the seizure focus and quantify their concordance with epileptiform transients, with which they are strongly associated. The patients were selected because interictal spikes were found within and outside the seizure onset zone. Visual inspection was used to identify and classify the ripples and FRs according to their relation to epileptiform spikes. Continuous-time wavelet analysis was used to compute their power. Ripples were present in all patients while FRs where found in five of the seven patients. Most ripples and FRs occurred at the same time as epileptiform transients. The rate of occurrence of ripples was higher within the seizure onset zone than outside in four of seven patients. The rate of FRs was much higher within the seizure onset zone than outside in four of the five patients with FRs (in these four patients, FRs were almost inexistent outside the seizure onset zone). The power of ripples and FRs tended to be higher in the electrodes where their rate was also higher. These results indicate that FRs were more restricted to the electrodes located within the seizure onset zone, especially to the hippocampus, than ripples. In only one patient, FRs were more frequent outside the seizure onset zone; this patient was the only one with cortical dysplasia and the electrode with a high rate of FRs was inside the lesion. This study demonstrates that interictal ripples and FRs can be recorded with depth macroelectrodes in patients. Most occur at the time of epileptiform spikes but some are isolated. Ripples do not show a clear differentiation between the seizure onset zone and remote areas, whereas FRs have a higher rate and higher power in the seizure onset zone. Our results also suggest a special capacity of the abnormal hippocampus to generate FRs, although they were also recorded in other structures.

Keywords: intracerebral EEG; ripples; fast ripples; high-frequency oscillations; spikes

Abbreviations: HFOs = high-frequency oscillations; FR = fast ripples; SEEG = stereoelectroencephalographic

Received March 8, 2007. Revised May 17, 2007. Accepted May 31, 2007. Advance Access publication July 11, 2007

Introduction

Recent findings suggest that changes in high-frequency activity in epileptic brains could have a central role in the process of epileptogenesis and seizure genesis. Interictal very high-frequency oscillations (HFOs), called fast ripples (FR) and ranging between 250 and 500 Hz, have been recorded from kainic acid-treated rats with chronic seizures and from epileptic patients (Bragin *et al.*, 1999*b*). They have been related to epileptogenesis (Engel *et al.*, 2003). Bragin and collaborators, studying recordings realized through microwires implanted with clinical depth electrodes in the mesial temporal structures of epileptic patients, described the presence of FR during the interictal period predominantly in the hippocampus ipsilateral to the seizure onset (Bragin *et al.*, 1999*b*, 2002*a*; Staba *et al.*, 2002). Although in early studies the relation between epileptic spikes in the EEG and FRs was not clear (Bragin *et al.*, 1999b), in later studies it was shown that most FRs appear at the same time as spikes (Engel *et al.*, 2003). The rate of FR occurrence was also higher during NREM sleep than during wakefulness or REM sleep (Bragin *et al.*, 1999*a*; Staba *et al.*, 2002, 2004).

To the best of our knowledge, the presence of interictal FRs in epileptic neocortex has not been reported, in animals or in patients, although we have reported changes in the high-frequency content of the EEG immediately following spikes (Urrestarazu *et al.*, 2006).

These interictal oscillations have been differentiated from the HFOs called ripples that have been recorded from normal hippocampus. Ripples range in frequency from 100 to 250 Hz in the hippocampus and entorhinal cortex of normal rats (Chrobak and Buzsaki, 1996; Chrobak *et al.*, 2000; Draguhn *et al.*, 2000), and from 80 to 160 Hz in the less abnormal hippocampus and entorhinal cortex of epileptic patients (Bragin *et al.*, 1999*a*). They have been interpreted as normal activity and it has been hypothesized that ripples could be part of mechanisms of memory consolidation (Draguhn *et al.*, 2000; Ponomarenko *et al.*, 2003). In control rats, ripples tend to occur in the middle of the normal sharp waves of the hippocampus (Bragin *et al.*, 1999b). The rate of occurrence of ripples is also higher during NREM sleep than during wakefulness or REM sleep (Staba *et al.*, 2004). It is notable that physiological high frequencies, even higher than 500 Hz, have been also described in the neocortex of cats (Grenier *et al.*, 2001) and in response to somatosensory stimulation in humans (Curio *et al.*, 1997), and they have been related to sensory information processing (Gobbele *et al.*, 2004; Hashimoto, 2000).

Changes in high-frequency activity have also been described in ictal recordings. HFOs in the range of 70 to 130 Hz have been described in the early phase of seizure discharges in patients with cortical malformations and dysplasias (Allen *et al.*, 1992; Fisher *et al.*, 1992). Recently, our group, using EEG macroelectrodes, recorded ictal HFOs between 100 and 500 Hz, preferentially from the seizure onset zone in mesial temporal and neocortical human epilepsies (Jirsch *et al.*, 2006).

We report here interictal HFOs recorded with intracranial macroelectrodes in patients with refractory focal epilepsy. We characterize their relation to the seizure focus and quantify their concordance with epileptiform transients. We were particularly interested in studying the differences between the HFOs recorded from the seizure onset zones and those generated outside the seizure onset zone.

Patients and Methods

Patient selection

Twenty-seven consecutive stereoelectroencephalographic (SEEG) studies realized between September 2004 and June 2006 in patients with medically refractory focal seizures undergoing pre-surgical investigation were visually reviewed. The SEEG studies were performed when comprehensive noninvasive pre-surgical evaluation yielded inconclusive results. The sites of electrode placement were individualized according to clinical history, seizure semiology, neuroimaging and surface EEG investigations. Since we were interested in how HFOs could localize the epileptogenic region, we selected patients in whom the following criteria were fulfilled: all seizure onsets involved the same region; seizure onset well localized; spikes present in regions within and outside the seizure onset zone during sleep, since fast ripples have been demonstrated mostly during epileptic spikes and studied during sleep (Engel, Jr *et al.*, 2003; Staba *et al.*, 2004). Eight of the 27 patients fulfilled these criteria. All had complex partial seizures, some with secondary generalization.

The Montreal Neurological Institute and Hospital Research Ethics Committee approved this study and informed consent was obtained from each patient.

Recording methods

SEEGs were acquired using the Harmonie long-term monitoring system (Stellate, Montréal, Canada). The implantation method consisted of a combination of intracerebral depth and cortical surface electrodes according to the methods described by Olivier and colleagues (Olivier *et al.*, 1994).

Intracerebral electrodes were manufactured on site by wrapping 3/1000 inch stainless steel wire around a 10/1000 inch stainless steel central core. These wires were coated with Teflon except for regions where the insulation was stripped to form electrode contacts. In total, there were nine contacts on each depth electrode bundle that were spaced along the length of the core wire at 5 mm intervals. The deepest contact (contact 1) was made from the tip of the core wire and had a non-insulated length of 1 mm, while the more superficial contacts (contacts 2 to 9) were formed from stripped sections of the marginal wire that was tightly wound to make 0.5 mm long coils. The effective surface area for contacts 2 to 9 was 0.80 mm^2, and it was 0.85 mm^2 for contact 1. Electrode bundles were implanted stereotactically using an image-guidance system (SSN Neuronavigation System, Mississauga, Ontario, Canada) through percutaneous holes drilled in the skull.

The SEEG was low-pass filtered at 500 Hz and sampled at 2000 Hz. The analysis was performed in a bipolar montage. Each channel compared two adjacent contacts of the same electrode bundle. Electrooculogram (EOG) and chin electromyogram (EMG) were also recorded to facilitate sleep staging.

Sleep staging and sample selection

The analysis below was only performed during periods of slow-wave sleep. Previous studies with microelectrodes demonstrated that high-frequency oscillations were much more frequent in non-REM sleep (Staba *et al.*, 2004). The standard Rechtschaffen and Kales criteria for defining sleep stages could not be used because we could not place central electrodes (the scalp is under a sterile bandage). As we could not be confident in separating stages 1 and 2 from wakefulness, we concentrated on stages 3 and 4. We used the following procedure to obtain EEG samples most likely to be from stages 3 and 4. For each patient, the SEEG recording from one night at least 24 h after the last seizure was selected. In a rapid visual review of several segments of the SEEG, the 2 or 3 channels showing the slow waves of highest amplitude (those considered related to sleep) were selected for trend analysis. Channels located in different regions were included. To identify sections of slow-wave sleep, spectral trends in the delta, alpha and beta bands were displayed for these intracranial channels and for the chin EMG, for the entire night with a 30-s time resolution (Harmonie, Stellate, Montreal, Canada). Segments with a high EEG power in the delta band and a low power in the EMG channel were visually reviewed to confirm the sleep stage.

Table 1 Demographic, neuroimaging and electrophysiological data of the seven patients

Patient	Age/gender	MR neuroimaging	Scalp EEG	Electrodes in SOZ	Electrodes outside SOZ
1	25 M	Neurocysticercosis, L Post. T gliosis and cyst	Interictal: LT Ictal: diffuse	LTP	LOF, LCi
2	34 F	MRI and interictal FDG PET, normal	Interictal: RT Ictal: RT	RA, RH	ROF
3	43 M	MRI normal	Interictal: no Ictal: L	LA, LH	LTPo
4	29 M	Bil. Mesial T atrophy, R>L	Interictal: T Ictal: L	RA, RH	LA, LH
5	46 M	Malrotation RH	Interictal: BT Ictal: BT	RA, RH	LA, LH, LATN,LMTN
6	51 M	Dysplasia LC (2nd Fr circumvolution)	Interictal: LCP Ictal: artifact	LSM, LIM	LSPC, LIPC
7	25 F	HHE, enlargement of R lateral ventricle	Interictal: RFT Ictal: RT	RA, RH	RATN, RMTN, RPTN

Note: Abbreviations: M, male; F, female; R, right; L, left; Bil., bilateral; Post., posterior; A, amygdala; ATN, anterior temporal neocortex; BT, bitemporal; C, central; Ci, cingulate; CP, centro-parietal; Fr, frontal; FT, fronto-temporal; H, hippocampus; IM, inferior motor area; IPC, inferior postcentral area; MTN, mesial temporal neocortex; OF, orbitofrontal; PTN, posterior temporal neocortex (Heschl gyrus); SM, superior motor area; SPC, superior postcentral area; T, temporal; TP, temporo-parietal; TPo: temporal pole; HHE, Hemiconvulsion-hemiparesis-epilepsy syndrome.

Slow-wave sleep was defined by the presence of more than 25% delta activity in SEEG channels by visual inspection in 30-s epochs.

In one patient the background activity consisted of continuous slow delta activity of moderate amplitude and slow-wave sleep could not be identified; this patient was therefore excluded from the study. The demographic, neuroimaging and electrophysiological data of the seven patients included in the study are shown in Table 1.

Selection and categorization of oscillations

Channels with spikes were identified using the bipolar montage described above and were classified as being within the seizure onset zone (SOZ) or outside the SOZ (Table 1). The SOZ was defined by the clinical electroencephalographer independently of this study. When a spike was recorded simultaneously over several channels of the same electrode bundle, only the channel showing the spike of highest amplitude was selected for analysis. When independent spikes were recorded in the same electrode bundle but in different channels, these spikes were analysed separately.

To visualize oscillations, the channel containing the spikes was displayed with the maximum time resolution, corresponding to ~0.6 s across the computer monitor (approximately 1200 samples of a signal sampled at 2000 Hz), and digitally high-pass filtered at 80 and at 250 Hz using a finite impulse response (FIR) filter. An FIR filter was used to eliminate ringing. Oscillations were visually identified and marked, specifying the onset and end points. Distinct oscillations were defined as events containing at least four consecutive peaks. Oscillations separated by 8 ms or more were considered different. Ripples and FR were marked independently of each other. The choice of 8 ms is arbitrary but was felt adequate as it represented a clearly visible interval, corresponding to a full period of an oscillation at 125 Hz, and more than a cycle for higher frequency oscillations.

To identify ripples, the computer screen was split in order to inspect simultaneously the expanded SEEG without filters and high-pass filtered at 80 Hz. Each ripple was classified in one of the following groups: (a) ripple visible during a spike (R-Vis-S), when the ripple could be seen superimposed on the spike in the unfiltered SEEG and was confirmed in the filtered SEEG (Fig. 1A); (b) ripple not visible during a spike (R-NVis-S), when no ripple could be seen on the original spike but the ripple was only obvious after filtering (Fig. 1B); and (c) ripple visible in the SEEG and confirmed in the filtered signal but not associated with a spike (R-Vis) (Fig. 1C).

To identify FRs, the computer screen was split to show the SEEG with the high-pass filter at 80 and at 250 Hz simultaneously, in addition to the original, unfiltered, EEG. The FRs were classified as: (a) fast ripple visible during a spike (FR-Vis-S); (b) fast ripple not visible during a spike (FR-NVis-S); and (c) fast ripple visible not associated with a spike (FR-Vis). The definitions are parallel to those of ripples and examples are shown on Fig. 2.

Rate of occurrence of oscillations

For each patient, the total rate of ripples and FRs and the rate of each of the six categories of events (R-Vis-S; R-NVis-S; R-Vis; FR-Vis-S; FR-NVis-S and FR-Vis) were calculated for each channel by dividing the number of events in that channel by the duration of EEG analysed.

To calculate the rate of events within the SOZ or outside the SOZ, the rates for all the channels in a zone were averaged. The rate of events in each patient was also estimated averaging the rates for all the channels of the same patient.

Measurement of frequency band power by spectral analysis

Continuous wavelet analysis was performed on EEG events using the Wavelet Toolbox available from Mathworks (Natick, Massachussets, USA). The complex Morlet wavelet was used to compute the power of EEG data in three frequency bands: gamma (30–80 Hz), ripple (80–200 Hz) and FR (250–450 Hz).

Statistical analysis of power data

Power differences were assessed between ripples within the SOZ and outside the SOZ using the Student's unpaired *t*-test.

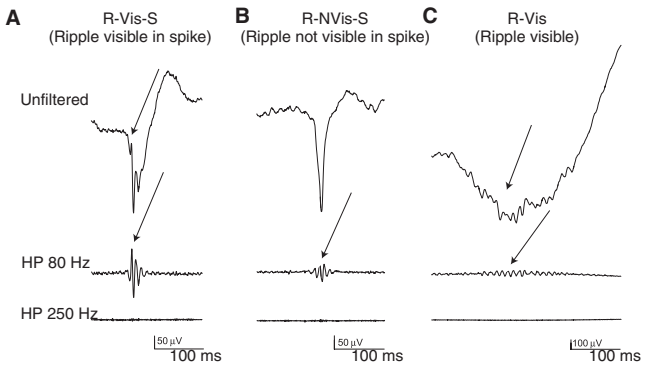

Fig. 1 Ripple classification. (**A**) Ripple visible in spike; (**B**) Ripple not visible in spike; (**C**) Ripple visible, independently of a spike. Top: non-filtered EEG; middle: EEG filtered with high pass filter of 80 Hz; bottom: EEG filtered with high-pass filter of 250 Hz.

Power differences were also assessed between R-Vis-S, R-NVis-S, R-Vis categories using an ANOVA for independent samples; *post hoc* comparisons were done using Scheffe's method. A maximum of 50 ripples per category and channel, randomly selected among the visually marked ripples, were used for this statistical analysis. A similar analysis was done for FRs.

Results

We analysed oscillations in 28 channels as a result of the selection criteria indicated above. Thirteen were classified as within the SOZ (mean 1.9/patient; range, 1–2). The small number of channels per patient originates from the selection of patients with a single and focal seizure type and from the fact that we analysed only the channel with the highest amplitude spike when spikes were present on multiple channels of the same electrode bundle. The other 15 channels were classified as outside the SOZ (mean 2.1/patient; range, 1–4). Here again the number of channel was low because spiking regions outside the focus are not frequent in patients with a single focal seizure onset, and the same channel selection based on spike amplitude was used as for the SOZ channels. The mean duration of the slow-wave sleep sections subjected to analysis was 18 min (range, 11–28). The visual marking of ripples and FRs was very time consuming: between 15 min and 15 h to mark one type of event, ripple or FR, for 10 min of a single channel of EEG. The longer time was for channels with many events.

Ripples

Ripples were seen in every patient and in 26 of 28 channels. Taking into account all patients, a total of 7123 ripples were detected. The rate of ripples in each patient ranged from 0.4 to 41/min (median, 14). The rate per channel ranged from 0 to 80/min (median, 4). Ripples were recorded from all studied areas, although the rate was much higher in mesial temporal structures than in neocortex (Fig. 3A).

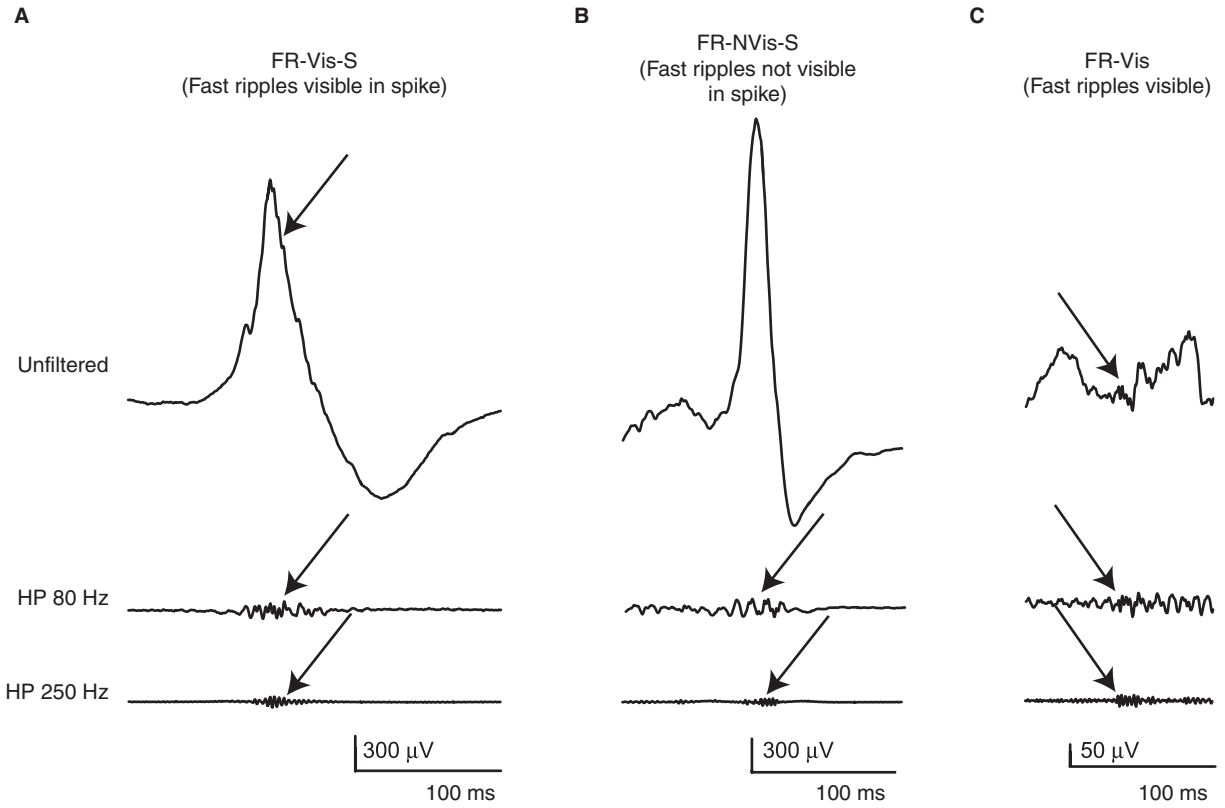

Fig. 2 Fast ripple classification. (**A**) Fast ripple visible in spike; (**B**) Fast ripple not visible in spike; (**C**) Fast ripple visible, independently of a spike. Top: non-filtered EEG; middle: EEG filtered with high-pass filter of 80 Hz; bottom: EEG filtered with high-pass filter of 250 Hz.

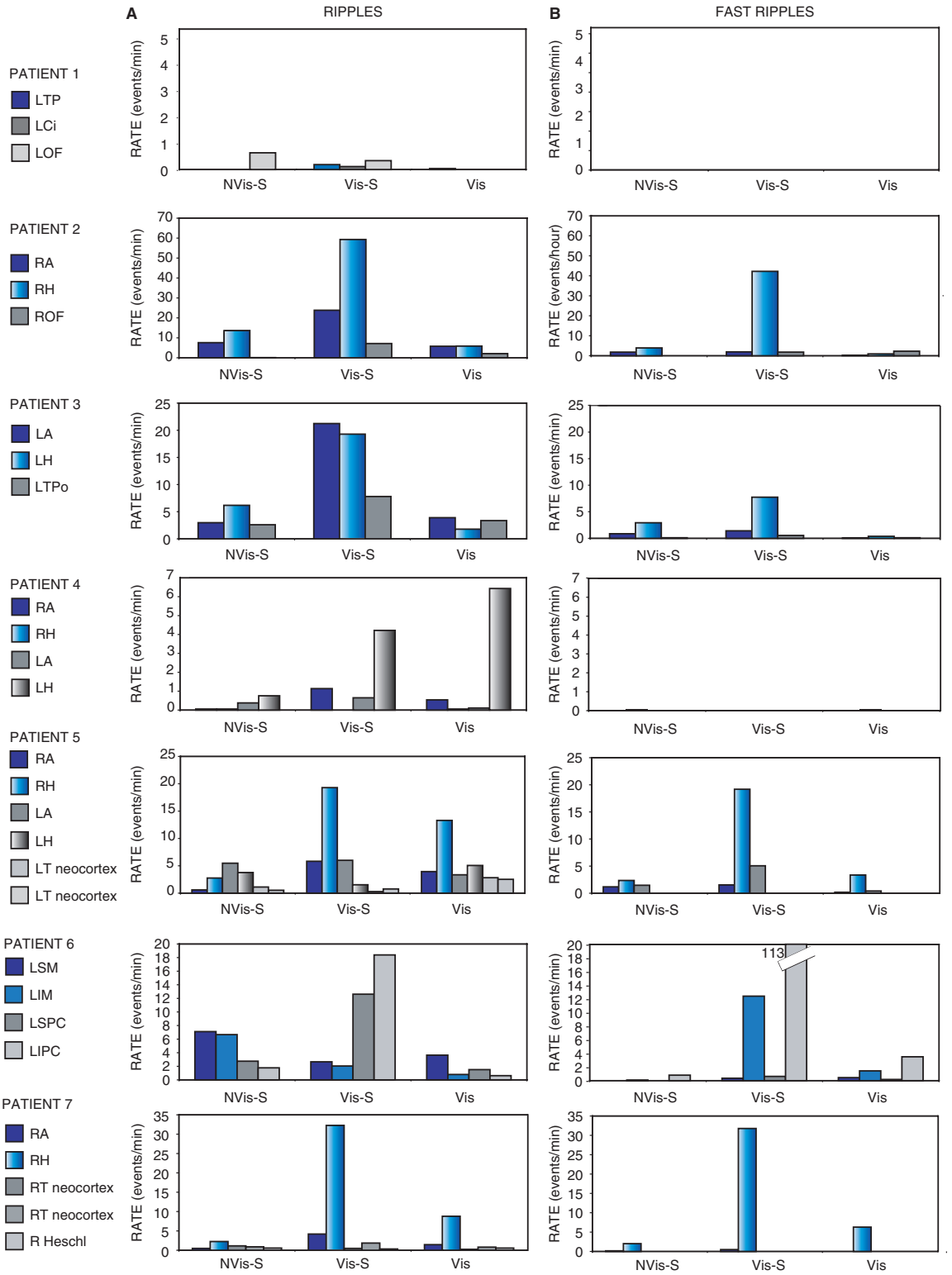

Fig. 3 Rate of occurrence of ripples and FRs in all analyzed channels. (**A**) Ripples. (**B**) Fast ripples. Each bar represents the rate of ripples or FRs in the corresponding channel. Channels located within the SOZ are represented in blue. Channels located outside the SOZ are represented in grey. Ripples have a more diffuse distribution than FRs, being present in most of the studied channels. FRs are restricted to few channels, and in four patients FRs are located mainly in the hippocampus. In most of the channels the rate of Vis-S categories are higher than the rate of NVis-S and Vis categories, both in ripples and FRs. R, right; L, left; A, amygdala; Ci, cingulate; H, hippocampus; IM, inferior motor area; IPC, inferior postcentral area; NVis-S: no visible in spike; OF, orbitofrontal; SM, superior motor area; SPC, superior postcentral area; T, temporal; TP, temporo-parietal; TPo, temporal pole; Vis: visible; Vis-S: visible in spike.

Comparison between ripple categories

Sixty-four percent of ripples were visible events during a spike or epileptiform sharp wave (R-Vis-S, Fig. 4; many examples are shown as this is the most common pattern). Nineteen percent did not coincide with any spike (R-Vis, Fig. 5D–F) and 17% corresponded to spikes without visible fast oscillations in the non-filtered recording (R-NVis-S, Fig. 5A–C). The ANOVA comparing the power in the three categories of ripples indicated a significant effect ($F = 198.8$, df = 2, $P < 0.001$). *Post hoc* comparisons revealed that power was significantly higher in the R-NVis-S category (mean ± SD, $47.5 \pm 6.4\ \mu V^2/Hz$) than in R-Vis-S category ($44.4 \pm 5.7\ \mu V^2/Hz$), while the R-Vis category was significantly lower than the other two ($41.9 \pm 5.1\ \mu V^2/Hz$). The ANOVA comparing the duration in the three categories of ripples indicated a significant effect ($F = 55$, df = 2, $P < 0.001$). *Post hoc* comparisons revealed that the duration of the R-NVis-S category (74.0 ± 53.8 ms) was significantly shorter than the duration in the R-Vis-S (98.6 ± 69.6 ms) and R-Vis (105 ± 67.6 ms) categories. The difference between the last two categories was not significant.

Comparison between within and outside the SOZ

In one of the seven patients, the ripples were localized exclusively outside the SOZ and in the remaining six patients they were located outside and within the SOZ. The rate of occurrence of the ripples within the SOZ ranged from 0 to 80/min (median, 6/min) and the rate outside the SOZ ranged from 0.1 to 21/min (median, 4/min). Figure 3A shows the rate in each channel for all patients. The rate within the SOZ, averaging the rates of all the channels located in the SOZ of each patient, ranged from 0 to 58/min (median, 23/min) and the rate outside the SOZ ranged from 0.6 to 19/min (median, 8/min). The rate was higher within than outside the SOZ in four patients. The results were the same if only the R-Vis-S category, the most common, was compared (rather than summing the three categories of ripples). Taking into account only the R-NVis-S category or only the R-Vis category, the rate was higher within than outside the SOZ also in four patients but not exactly in the same patients. Histograms of Fig. 6A show the rate ratio between within and outside the SOZ for each patient. Histograms of Fig. 6B show the same ratio taking into account only the R-Vis-S category.

The mean power of the ripples within the SOZ ranged from 37.8 to 49.6 $\mu V^2/Hz$ (mean ± SD, 44.2 ± 4.5), and from 36.9 to 50.4 $\mu V^2/Hz$ outside the SOZ (43.3 ± 4.0). The power was significantly higher within the SOZ than outside the SOZ in four patients. These four patients coincided with the patients in whom the rate was higher within than outside the SOZ. On the other hand, the power

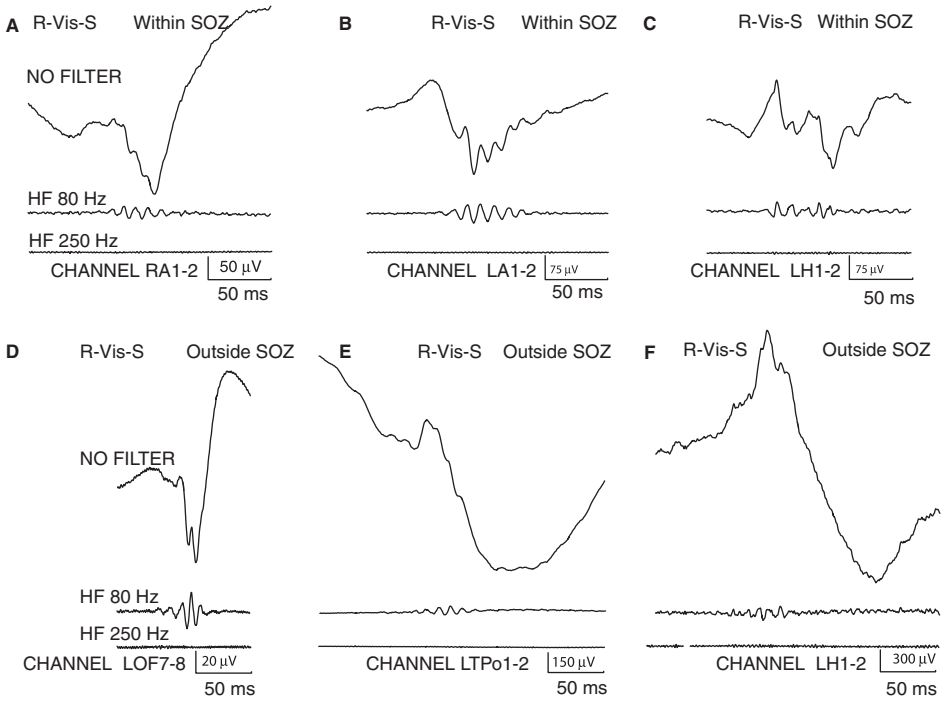

Fig. 4 Examples of ripples visible during spikes. (**A**, **B** and **C**) Ripples within the SOZ, with different levels of morphological regularity. (**D**, **E** and **F**) Ripples outside the SOZ, also showing different levels of morphological regularity. Top: non-filtered EEG; middle: EEG filtered with high-pass filter of 80 Hz; bottom: EEG filtered with high-pass filter of 250 Hz. L, left; R, right; A, amygdala; H, hippocampus; OF, orbitofrontal cortex; TPo, temporal pole. The ripples visible during spikes have similar morphological characteristics independently of being within or outside the SOZ, in mesial temporal lobe or in temporal and extratemporal neocortex. Some of these ripples are irregular oscillations.

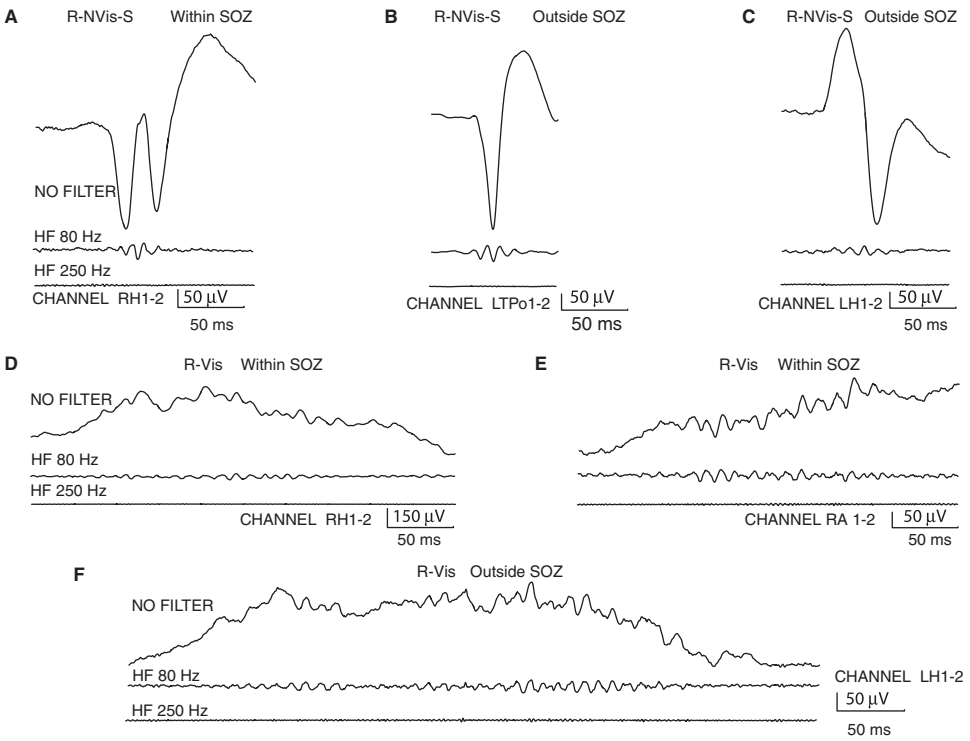

Fig. 5 Examples of ripples no visible during spikes and ripples visible independently of spikes. (**A**) Ripple not visible during spike located within the SOZ. (**B** and **C**) Ripples not visible during spike located outside the SOZ. (**D** and **E**) Ripples visible independently of a spike located within the SOZ. (**F**) Ripple visible located outside the SOZ. Top: non-filtered EEG; middle: EEG filtered with high-pass filter of 80 Hz; bottom: EEG filtered with high-pass filter of 250 Hz. L, left; R, right; A, amygdala; H, hippocampus; TPo, temporal pole. The morphological characteristics of the ripples no visible during spikes located within the SOZ and the ones located outside the SOZ are similar. This similarity is also seen between ripples visible independently of a spike within and outside the SOZ. Some of these ripples are irregular oscillations.

was significantly higher outside SOZ than within the SOZ in three patients (including the patient with ripples exclusively outside the SOZ), who also were the same patients in whom the rate was higher outside than within the SOZ (see histograms Fig. 6A and B bottom).

Ripple duration was significantly longer within than outside the SOZ in three patients and significantly shorter in one patient. In two patients there were no significant differences between within and outside the SOZ. In the remaining patient ripples were exclusively located outside the SOZ.

Fast ripples

FRs were seen in five of the seven patients (patients #2, 3, 5, 6, 7). All the results in this section will refer to these five patients. A total of 4081 FRs were detected. In four patients most of the FRs were overlapping with ripples (range: 67–97%; median: 91%). Most of them were completely enclosed, i.e. starting after the start of a ripple and finishing before the end of that ripple (range, 55–91%; median, 72%). In the remaining patient more than 85% of the FRs were not enclosed in the R. The rate of FRs in each patient ranged from 0.3 to 33/min (median, 5). The rate per channel ranged from 0 to 118/min (median, 2.3/min). FRs were spatially less diffusely distributed than R. In these five patients, FRs were recorded in 16 of 21 analysed channels (76%) while ripples were recorded in all the 21 analysed channels. As with the ripples, their rate was much higher in the mesial temporal structures, mainly in the hippocampus, than in neocortex (Fig. 3B). The five channels that recorded ripples but did not record FRs were located in temporal neocortex (four channels) and Heschl gyrus (one channel).

Comparison between FR categories

Eighty-six percent of FRs were visible events during a spike or epileptiform sharp wave (FR-Vis-S, Figs. 7 and 8A, B, E; many examples are shown as this is the most common pattern). Eight percent of FR did not coincide with any spike (FR-Vis, Fig. 8B and D) and 6% corresponded to spikes without visible fast oscillations in the non-filtered recording (FR-NVis-S, Fig. 8C). The ANOVA comparing the power in the three categories of fast ripples indicated a significant effect ($F = 52.66$, $df = 2$, $P < 0.001$). *Post hoc* comparisons revealed that the power of the fast ripples was significantly higher in the FR-NVis-S

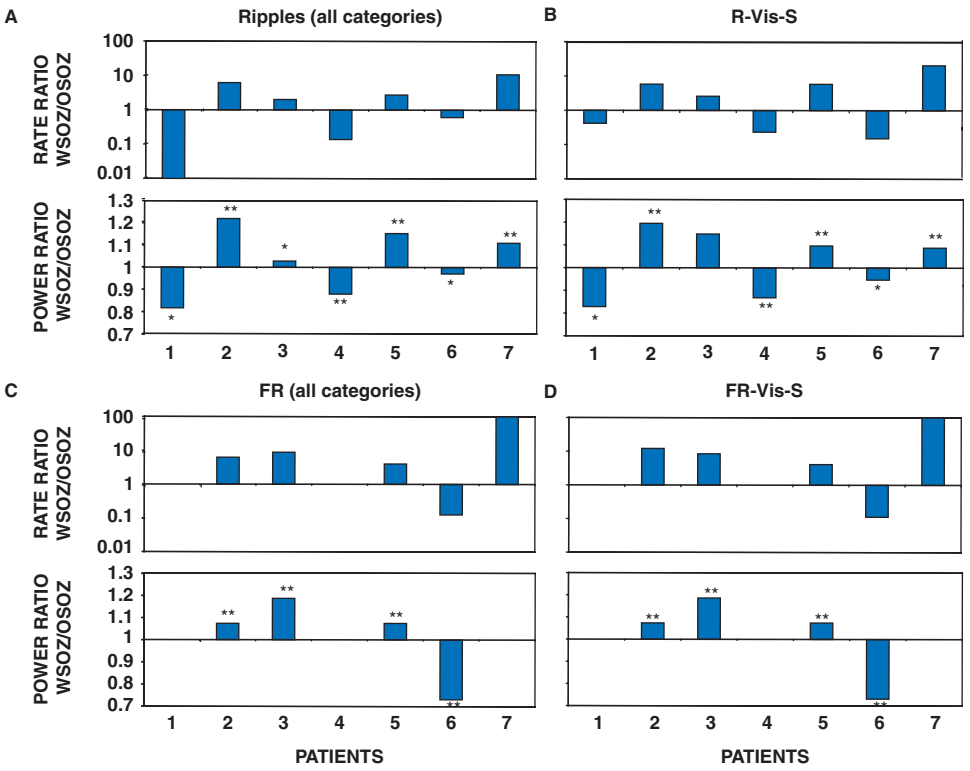

Fig. 6 Rate ratio (top) and power ratio (bottom) between within and outside the SOZ of all ripples and FRs and of R-Vis-S and FR-Vis-S categories, for each patient. (**A**) Ripples of all categories; (**B**) ripples of the R-Vis-S category; (**C**) fast ripples of all categories; (**D**) fast ripples of the FR-Vis-S category. The horizontal scale represents each patient. The rate ratio is shown in a logarithmic scale. Values of this ratio >100 or <0.01 indicate unilateral events. The level of statistical significance in the difference of ripple power between the SOZ and outside the SOZ is shown as * for $P<0.05$ and ** $P<0.001$. Similarly for FRs. WSOZ: within SOZ; OSOZ: outside SOZ. A higher rate of occurrence and higher power of ripples corresponds to the SOZ in four patients and to outside the SOZ in three patients. A higher rate of occurrence and higher power of FRs corresponds to the SOZ in four of the five patients with FRs. The same results are found using only the ripples visible during spikes or FRs visible during spikes.

category ($33.4 \pm 5.6\,\mu V^2$/Hz) than in FR-Vis-S category ($31.0 \pm 5.9\,\mu V^2$/Hz), while in the FR-Vis category it was significantly lower than in the other two ($28.6 \pm 3.7\,\mu V^2$/Hz). The ANOVA comparing the duration in the three categories indicated a significant effect ($F=6.5$, df = 2, $P<0.005$). *Post hoc* comparisons revealed that the duration of the FR-NVis-S category (40.3 ± 20.5 ms) was significantly shorter than the duration in the FR-Vis-S (47.0 ± 20.0 ms). There were no significant differences between FR-Vis (45.2 ± 27.0 ms) and the other two categories.

Comparison between within and outside the SOZ

In one of the five patients the FRs were localized exclusively within the SOZ (none were found outside the SOZ) and in the remaining four patients they were found within and outside the SOZ. The rate of occurrence of FRs in channels within the SOZ ranged from 0.6 to 48/min (median, 8/min) and the rate in the channels outside the SOZ ranged from 0 to 118/min (median, 0.1/min). The very low median outside the SOZ originates from the fact that five channels have no FRs at all and most channels have a low rate of FR occurrence; only one channel has the very high rate of 118 FR/min. Figure 3B shows the rate in each channel for all the patients. The rate of FR within the SOZ, including all the channels located in each such zone, ranged from 7 to 26/min (median, 14/min) and the rate outside the SOZ ranged from 0.8 to 59/min (median, 3/min). Comparing the rates within and outside the SOZ, the rate of FR was higher within than outside the SOZ in four of the five patients (including the patient with FRs found exclusively within the SOZ). In one patient the rate of FR was higher outside than within the SOZ. The result was the same if only the FR-Vis-S or the FR-NVis-S categories were compared. Taking into account only the FR-Vis category, the rate was higher within than outside the SOZ in three patients and the rate was higher outside than within the SOZ in the other two. The histograms of Fig. 6C (top) show the rate ratio between within and outside the SOZ for each patient. The histograms of Fig. 6D (top) show the rate ratio taking into account only the FR-Vis-S category.

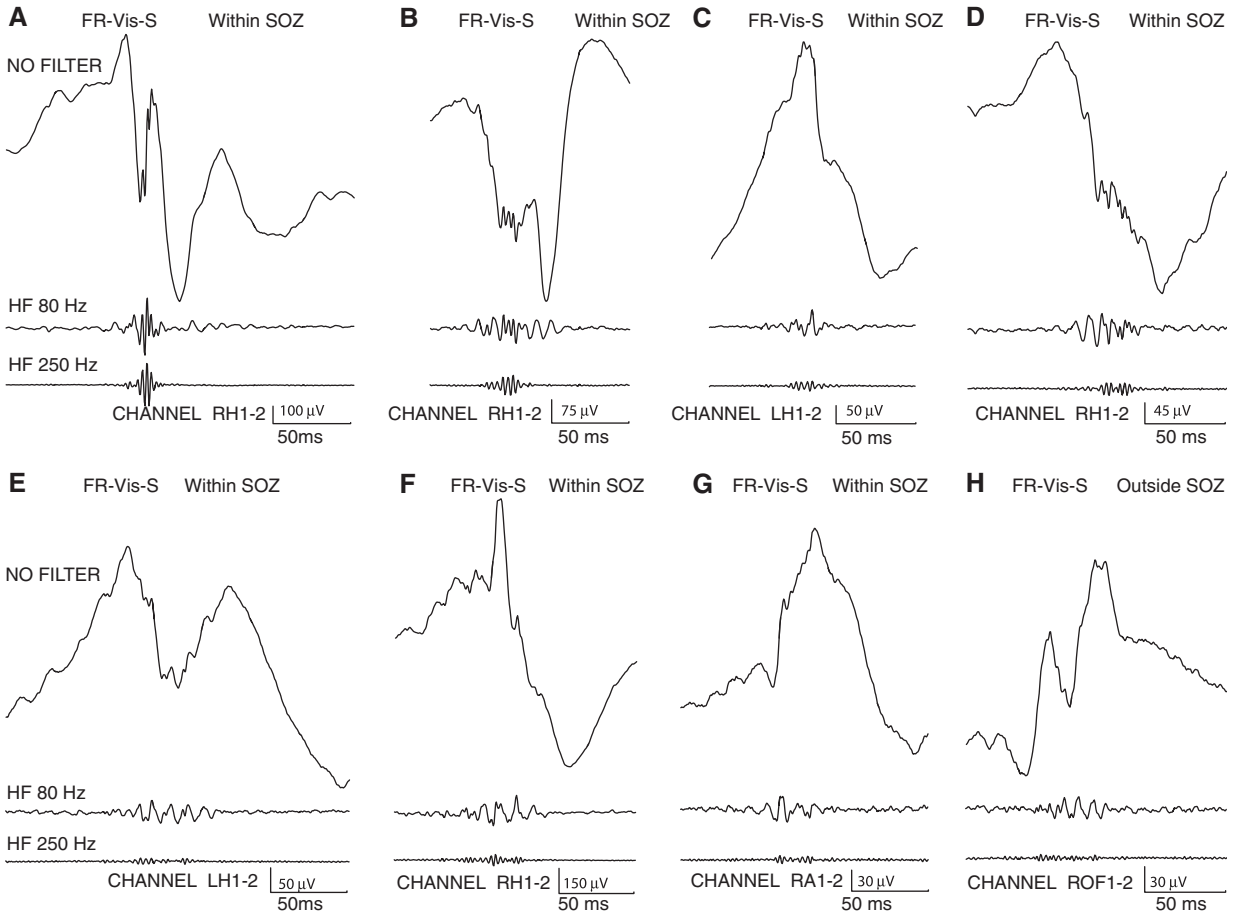

Fig. 7 Examples of fast ripples visible during spikes. (**A**) FR-Vis-S not overlapping with a ripple located within the SOZ; (**B–G**) FR-Vis-S overlapping with ripples, located within the SOZ; (**H**) FR-Vis-S overlapping with a ripple, located outside the SOZ. L, left; R, right; A, amygdala; H, hippocampus; OF, orbitofrontal cortex. Most of the FRs visible during spikes are intermingled with ripples, sometimes at the beginning (**B**), during (**C**) or at the end (**D**) of the ripple. The morphological characteristics of the FRs visible during spikes located outside the SOZ and neocortex are similar to the more usual FRs located inside the SOZ and hippocampus.

The mean power of the FR within the SOZ ranged from 21.3 to 34.0 μV^2/Hz (mean $\pm$ SD, 29.8 $\pm$ 5.0), and from 26.2 to 31.0 μV^2/Hz outside the SOZ (28.1 $\pm$ 1.9). The power was significantly higher within the SOZ than outside the SOZ in four of the five patients with FRs. A power comparison cannot be formally performed in the patient having FRs only within the SOZ, but we consider that power within the SOZ is higher than outside the SOZ, where it is zero. These four patients were the same as the patients in whom the rate was higher within than outside the SOZ. On the other hand, the power was significantly higher outside than within the SOZ in the remaining patient, who was also the patient in whom the rate of FR occurrence was higher outside than within the SOZ (see histograms Fig. 6C and D, bottom).

The FR duration was significantly longer within the SOZ in two patients and significantly longer outside the SOZ in the other two patients with FR within and outside the SOZ.

Location of ripples and FRs

Ripples were found in all the regions studied, including mesio-temporal and neocortical areas. They were also found in the different lesion types present in our patients as well as in regions without MRI abnormality. As indicated above, they were not preferentially found in the region of seizure onset.

FRs were not found in one patient with a posterior temporal cystic lesion (patient #1) and in one patient with bilateral mesio-temporal atrophy (patient #4). They were found in two patients with no MRI abnormality, in one with a hippocampal malformation and in one with right hemisphere atrophy (patients #2, 3, 5 and 7, see Table 1). In these four patients, FRs were found predominantly in the hippocampus, but also in the amygdala and neocortex, and FRs predominated in the SOZ. In the fifth patient with FRs (patient #6), the only one with cortical dysplasia, FR were present in the SOZ with a rate similar to that seen in the SOZ of the other four patients (Fig. 3B), but they

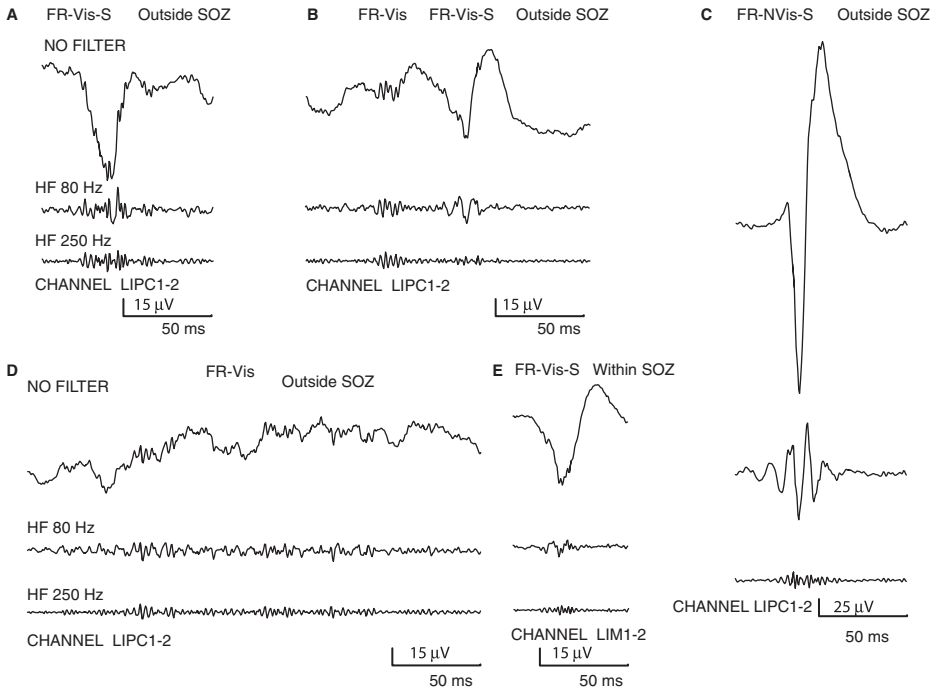

Fig. 8 Examples of fast ripples recorded in patient #6, with cortical dysplasia. (**A–D**) Outside the SOZ. (**E**) Within the SOZ. Top: non-filtered EEG; middle: EEG filtered with high-pass filter of 80 Hz; bottom: EEG filtered with high-pass filter of 250 Hz. LIPC, left inferior postcentral area; LIM, left inferior motor area. The morphological characteristics of the FRs are similar between the different categories and within or outside the SOZ. In this patient most of the FRs were not associated to ripples.

were much more frequent outside the SOZ, in a region that was however part of the dysplastic cortex. Figure 8 shows examples of FRs found outside and within the SOZ in this patient.

Discussion

We have demonstrated that ripples and FRs can be recorded with macroelectrodes and are relatively frequent in the interictal period (median, 4/min/channel for ripples and 2.3/min/channel for FRs). Their main characteristics can be summarized as follows. Both occur most often riding on top of spikes (64% for ripples and 86% for FRs), although they can also be seen in the absence of spikes. A small minority is seen only as a result of filtering a spike and simply results from the fact that the spike is very sharp, and therefore includes high-frequency components. It could be argued that these events should be ignored as they do not represent a genuine oscillation. They represent the presence of a spike that is particularly sharp, and it is possible that this has its own importance. In any case, our results would not change significantly if these events are included or not. Ripples and FRs are also relatively long events: the mean duration is around 80 ms for ripples and 40 ms for FRs. Although there are some differences in energy between ripples and FRs that are riding on top of spikes and those occurring independently of spikes, the power is generally of the same order of magnitude (45 μV^2/Hz for ripples and 30 μV^2/Hz for FRs). The amplitude measure therefore does not indicate that these two types of oscillations have different origins. Finally, ripples and FRs are frequently overlapping.

When comparing the rate of occurrence of ripples and FR in our EEG recordings and those found in microelectrode recordings, it is remarkable that they are quite similar. Both studies were done during non-REM sleep (ours was more specifically in slow-wave sleep), thus ensuring a relative uniformity, although the variability of occurrence of ripples and FR needs to be systematically evaluated during the different sleep stages and during wakefulness. The rate for ripples recorded with microelectrodes in humans ranged from 0.1 to 20/min, being more often lower than 3–4/min; our median rate of occurrence for ripples was 4/min. The rate of FRs ranged from 0.5 to 20/min, being more often lower than 1–2/min, in microelectrode recordings (Bragin *et al.*, 1999*a*; Staba *et al.*, 2002, 2004); our median rate was 2.3/min. The median duration of the events recorded with microelectrodes were a little different depending on the study and ranged from 32 to 57 ms for ripples and from 15 to 25 ms for FRs (Bragin *et al.*, 2002*b*; Staba *et al.*, 2002). Our mean durations were 80 ms for ripples and 40 ms for FRs, somewhat longer but still very much of the same order of magnitude. It is not meaningful to compare amplitudes obtained with micro- and macroelectrodes, because they are dependent on the electrode type. Overall, the HFOs

measured with microelectrode and the EEG HFOs measured with macroelectrodes were of remarkably similar rate of occurrence and duration, reinforcing the possibility that they are the same events, observed by different means. We did not examine systematically the spatial extent over which simultaneous ripples or FRs could be observed. In casual observations we found that ripples were not infrequently seen simultaneously in two electrodes (separated by 5 mm). On the other hand, FRs were most often seen in one electrode only, except in the patient with a very high rate of occurrence, in whom they could be seen in two adjacent electrodes. A systematic study of the spatial extent of HFOs should be undertaken to determine if this extent has an impact on the epileptogenicity of the region.

Ripples were found in all seven patients and appear quite evenly distributed within and outside the SOZ, although there is a tendency for them to be more frequent within the SOZ (median rate 6/min/channel within SOZ and 4 outside). This applies to all different categories of ripples (on spikes or independent of spikes). This is in contrast with the ripples seen with microelectrodes, which were more frequent in the mesial temporal lobe contralateral to that of seizure onset (Staba *et al*., 2002) (it can be considered that, in that study, the mesial temporal lobe contralateral to that of seizure onset corresponds to what we call 'outside the SOZ', whereas the mesial temporal lobe of seizure onset corresponds to our 'inside the SOZ'). It must be noted, however that the difference between the two sides in the microelectrode study was not statistically significant, probably because of the high variability between subjects. This high variability was also present in our study and it appears that ripples are unlikely to be useful in individual subjects to determine if a region is more or less normal.

Fast ripples were not found in all patients (present in five of seven) but when present, their rate separates more clearly the SOZ (median rate 8/min/channel) from outside the SOZ (0.1/min/channel). The ratio of rates within the SOZ to that outside the SOZ was $6/4 = 1.5$ for ripples and $8/0.1 = 80$ for FRs. In fact, FRs are almost absent outside the SOZ with the exception of a very high rate in one of the five patients with FRs. In the four other patients, the median rate of occurrence of FRs is 8/min/channel within and 0/min/channel outside the SOZ. There appears to be as good or possibly a better separation between the SOZ and outside the SOZ with FRs recorded on EEG than with FRs recorded with microelectrodes (Bragin *et al*., 2002a; Staba *et al*., 2002). This may not, however, apply to all pathologies. It is noticeable that two patients had no FRs within the SOZ. It will be interesting to follow up all these patients after surgery, to assess if the epileptogenic zone corresponded to the seizure onset zone seen with our depth electrodes, and whether removal of the region including FRs was likely to lead to a favourable outcome.

Ripples and FRs have only been reported until now from mesial temporal structures, but only these structures have been investigated. We found ripples and FRs in mesial temporal and neocortical structures within and outside the temporal lobe, although with a much higher rate of occurrence in mesial temporal regions. They were also found in all the different types of pathology seen in this group of patients. One intriguing finding is the extremely high rate of FRs in the one patient with cortical dysplasia, outside the SOZ, although the SOZ also showed a high rate of occurrence (similar to that in the SOZ of other patients). This raises the possibility that this is a marker of cortical dysplasia, which would be an extension of the very high rate of EEG spiking seen in the scalp and intracerebral EEG in this pathology (Palmini *et al*., 1995; Gambardella *et al*., 1996; Chassoux *et al*., 2000).

HFOs have been reported in experimental animals and in humans, in microelectrode recordings. Their relationship with epileptogenicity appears quite solid, although no clear link between FRs and the actual generation of seizures has been established. Also, given the very small volumes over which they could be found, it was not clear that they could be recorded with EEG electrodes. In our case, the EEG electrodes have a surface contact approximately 700 times larger than the microelectrodes used in human studies. It can therefore be concluded that HFOs occur over a larger volume than could be assessed with microelectrodes (because the latter use a reference a few hundred microns from the active electrodes, they could not see a field encompassing the reference and the active electrodes). It is clear that the electrode size affects the ability to record from generators having a size similar to or smaller than the electrode contact. The optimum size of electrode required to see oscillations in the range of 100 to 500 Hz remains to be determined.

It is tempting to conclude that FRs are indicative of the region of seizure onset, but we must be cautious. This could be proven formally if two conditions could be fulfilled: removal of regions with FRs leads to seizure freedom and non-removal of regions with FRs leads to continued seizures. We do not have a sufficient number of patients and sufficient follow-up to answer these questions. Two of our seven patients did not show any FRs in what we considered the SOZ. Unless it turns out that, following removal of this region, they do not become seizure free, we do not have any indication that the SOZ must include FRs. Can we conclude that if FRs are present, one can be confident that the SOZ has been identified? Our data show frequent FRs in one patient outside the SOZ. Could it be that they represent a region of potential seizure onset, although none of the seizures recorded during the investigation started in that region? Here again, we would be on more solid ground if this patient' surgery did not include the region with FRs and if his seizure persisted. A long-term follow-up with a precise mapping of the surgical resections compared to the regions of FRs

generation will be necessary to conclude on the practical importance of FRs in determining the seizure generating region.

This study establishes, in conjunction with our earlier studies (Jirsch *et al.*, 2006; Urrestarazu *et al.*, 2006) the presence and significance of high-frequency activity in the intracerebral EEG of patients with epilepsy, pointing to the possible specific importance of FRs and opening new avenues in the clinical investigation of epileptic patients and in our understanding of epileptogenicity.

Acknowledgements

This project was supported by grant MOP-10189 from the Canadian Institutes of Health Research. We are grateful to Jeff Jirsch for his initial analysis of high-frequency interictal oscillations and for discussions of issues relating to their identification.

References

Addison PS. The illustrated wavelet transform handbook. Bristol: The Institute of Physics Publishing; 2001.

Allen PJ, Fish DR, Smith SJ. Very high-frequency rhythmic activity during SEEG suppression in. Electroencephalogr. Clin Neurophysiol 1992; 82: 155–9.

Bragin A, Engel J, Jr, Wilson CL, Fried I, Buzsaki G. High-frequency oscillations in human brain. Hippocampus 1999a; 9: 137–42.

Bragin A, Engel J, Jr, Wilson CL, Fried I, Mathern GW. Hippocampal and entorhinal cortex high-frequency oscillations (100–500 Hz) in human epileptic brain and in kainic acid—treated rats with chronic seizures. Epilepsia 1999b; 40: 127–37.

Bragin A, Mody I, Wilson CL, Engel J, Jr. Local generation of fast ripples in epileptic brain. J Neurosci 2002a; 22: 2012–21.

Bragin A, Wilson CL, Staba RJ, Reddick M, Fried I, Engel J, Jr. Interictal high-frequency oscillations (80-500 Hz) in the human epileptic brain: entorhinal cortex. Ann Neurol 2002b; 52: 407–15.

Chassoux F, Devaux B, Landre E, et al. Stereoelectroencephalography in focal cortical dysplasia: a 3D approach to delineating the dysplastic cortex. Brain 2000; 123 (Pt 8): 1733–51.

Chrobak JJ, Buzsaki G. High-frequency oscillations in the output networks of the hippocampal-entorhinal axis of the freely behaving rat. J Neurosci 1996; 16: 3056–66.

Chrobak JJ, Lorincz A, Buzsaki G. Physiological patterns in the hippocampo-entorhinal cortex system. Hippocampus 2000; 10: 457–65.

Curio G, Mackert BM, Burghoff M, et al. Somatotopic source arrangement of 600 Hz oscillatory magnetic fields at the human primary somatosensory hand cortex. Neurosci Lett 1997; 234: 131–4.

Draguhn A, Traub RD, Bibbig A, Schmitz D. Ripple (approximately 200-Hz) oscillations in temporal structures. J Clin Neurophysiol 2000; 17: 361–76.

Engel J, Jr, Wilson C, Bragin A. Advances in understanding the process of epileptogenesis based on patient material: what can the patient tell us? Epilepsia 2003; 44 (Suppl 12): 60–71.

Fisher RS, Webber WR, Lesser RP, Arroyo S, Uematsu S. High-frequency EEG activity at the start of seizures. J Clin Neurophysiol 1992; 9: 441–8.

Gambardella A, Palmini A, Andermann F, et al. Usefulness of focal rhythmic discharges on scalp EEG of patients with focal cortical dysplasia and intractable epilepsy. Electroencephalogr Clin Neurophysiol 1996; 98: 243–9.

Gobbele R, Waberski TD, Simon H, et al. Different origins of low- and high-frequency components (600 Hz) of human somatosensory evoked potentials. Clin Neurophysiol 2004; 115: 927–37.

Grenier F, Timofeev I, Steriade M. Focal synchronization of ripples (80-200 Hz) in neocortex and their neuronal correlates. J Neurophysiol 2001; 86: 1884–98.

Hashimoto I. High-frequency oscillations of somatosensory evoked potentials and fields. J Clin Neurophysiol 2000; 17: 309–20.

Jirsch JD, Urrestarazu E, LeVan P, Olivier A, Dubeau F, Gotman J. High-frequency oscillations during human focal seizures. Brain 2006; 129: 1593–608.

Misiti M, Misiti Y, Oppenheim G, Poggi JM, editors. Wavelet toolbox user's guide v3. Natick, MA: MathWorks; 2006.

Olivier A, Germano IM, Cukiert A, Peters T. Frameless stereotaxy for surgery of the epilepsies: preliminary experience. Technical note. J Neurosurg 1994; 81: 629–33.

Palmini A, Gambardella A, Andermann F, et al. Intrinsic epileptogenicity of human dysplastic cortex as suggested by corticography and surgical results. Ann Neurol 1995; 37: 476–87.

Ponomarenko AA, Korotkova TM, Haas HL. High frequency (200 Hz) oscillations and firing patterns in the basolateral amygdala and dorsal endopiriform nucleus of the behaving rat. Behav Brain Res 2003; 141: 123–9.

Staba RJ, Wilson CL, Bragin A, Fried I, Engel J, Jr. Quantitative analysis of high-frequency oscillations (80-500 Hz) recorded in human epileptic hippocampus and entorhinal cortex. J Neurophysiol 2002; 88: 1743–52.

Staba RJ, Wilson CL, Bragin A, Jhung D, Fried I, Engel J, Jr. High-frequency oscillations recorded in human medial temporal lobe during sleep. Ann Neurol 2004; 56: 108–15.

Urrestarazu E, Jirsch JD, LeVan P, et al. High-frequency intracerebral EEG activity (100-500 Hz) following interictal spikes. Epilepsia 2006; 47: 1465–76.

Appendix I

The Morlet wavelet ψ as a function of time t is defined as (Addison, 2001)

$$\psi(t) = e^{-t^2/2} e^{2j\pi f_0 t}$$

where f_0 represents the centre frequency of the mother wavelet and was set to 0.7958 Hz. The wavelet can be dilated in time by a scale a or translated in time by an offset b. This process produces daughter wavelets and is represented mathematically as (Misiti *et al.*, 2006)

$$\psi\left(\frac{t-b}{a}\right) = e^{-(1/2)[(t-b)/a]^2} e^{2\pi}[f_0(t-b/a)]$$

Let $x(t)$ represent the EEG data sample from a particular channel at time t. Let an event be defined by the instant of onset t_{onset} and the instant of end t_{end}

The complex wavelet coefficients C can be computed for a given scale a and offset b as follows (Misiti *et al.*, 2006)

$$C(a,b) = \frac{1}{\sqrt{a}} \int_{-\infty}^{\infty} x(t) \psi^* \left(\frac{t-b}{a}\right) dt$$

where the asterisk represents complex conjugation.

The power P contained in each event at a given scale a can be computed from the wavelet coefficients as follows:

$$P(a) = \int_{t_{onset}}^{t_{end}} \frac{|C(a,b)|^2}{t_{end} - t_{onset}} db \Bigg|$$

A scale a is related to a pseudo-frequency f of the daughter wavelet, according to the following relationship:

$$a(f) = \frac{f_0}{fT}$$

where T is the sampling period and is equal to 0.5 ms.

For the analysis, three frequency bands were defined, namely, Gamma (30–80 Hz), Ripple (80–200 Hz) and Fast Ripple (250–450 Hz). Discrete frequency values in each of the three bands were used to generate a scale-set A containing discrete scale values.

$$AG = a(f) \text{ for } f = 30, 35, 40, 45, 50, 70, 75, 80$$

$$A_R = a(f) \text{ for } f = 80, 85, 90, 95, 100, 105, 110, 130, 140, 150 \ldots 200$$

$$AFR = a(f) \text{ for } f = 260, 280, 320, 340, 380, 400, 440$$

As the wavelet's bandwidth increases with frequency, the frequency sampling interval was arbitrarily fixed at: 5 Hz from 30 to 110 Hz, 10 Hz from 130 to 200 Hz and 20 Hz from 200 to 440 Hz. The frequency samples corresponding to 60 Hz harmonics were rejected to reduce artefacts due to line noise. The power in the Gamma, Ripple and Fast Ripple bands was computed by summing the power over their corresponding scale-sets.

$$P_G = \sum_{A_G} P(a),\ P_R = \sum_{A_R} P(a),\ P_{FR} = \sum_{A_{FR}} P(a)$$

Consequently, the wavelet analysis for each event led to the computation of three values namely, P_{G}, P_{R}, and P_{FR}.